Effect of chemical structure of organics on pore wetting

OPEN ACCESS

Effect of chemical structure of organics on pore wetting

Xingxun Li [a], Hui Fan [b], Xianfeng Fan [a],*

[a] *Institute for Materials and Processes, School of Engineering, The University of Edinburgh, King's Buildings, Mayfield Road, Edinburgh EH9 3JL, United Kingdom*

[b] *College of Medical and Dental Sciences, The University of Birmingham, Birmingham B15 2TT, United Kingdom*

HIGHLIGHTS

- Contact angles of organics were measured in micron-sized pores.
- Chemical structure of organics does affect the contact angle in a glass pore.
- Contact angle of amphiphiles in a glass pore varies with functional group.
- Contact angle of amphiphiles in a glass pore increases with alkyl chain length.
- Side chain on the backbone carbon reduces the contact angle in a glass pore.

GRAPHICAL ABSTRACT

ABSTRACT

Pore wetting is significant for understanding fluid behaviour in porous media. In this paper, a range of organics with similar surface tensions were used to investigate the effect of chemical structure on g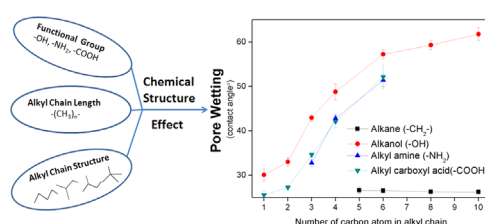lass pore wetting. We measured contact angles of organics in a single glass capillary. Our results indicate that the chemical structure of organics does significantly affect the contact angle in a single glass pore. The amphiphiles have similar surface tensions, but their contact angles vary greatly with their chemical structures. The amphiphiles with functional groups have larger contact angles than the non-polar organics, and in the order of $\theta_{-OH} > \theta_{-NH_2} \approx \theta_{-COOH}$. The contact angle of amphiphile in a glass pore increases with the straight alkyl chain length. The straight alkyl chain contributes to the pore contact angle most and the side chain on the carbon of backbone tends to reduce the pore contact angle. The symmetrical molecular structure gives the smallest contribution on the pore wetting. In addition, the contact angles of amphiphiles were also measured in a hydrophobic PMMA (poly(methyl methacrylate)) pore, and compared with those in a hydrophilic glass pore. The results indicate that the chemical structure has no contribution on hydrophobic pore wetting.

© 2015 Elsevier Ltd. All rights reserved.

1. Introduction

It is well known that pore wetting is of significance in many practical processes, such as fuel cells, groundwater movements, material engineering, nanofluidics, nanolubrication, CO_2 storage and oil recovery (Altman et al., 2014; Bikkina, 2011; Brovchenko and Oleinikova, 2011; Chalbaud et al., 2009; Espinoza and Santamarina, 2010; Hui and Blunt, 2000; Martic et al., 2005; Raimondo et al., 2014; Saraji et al., 2013; Sghaier et al., 2006; Stukan et al., 2010; Vanzo et al., 2014). For instance, the wettability of a porous-structured oil reservoir controls how and where fluids flow and reside in the reservoir and determines the displacement efficiency for oil recovery (Ersland et al., 2010). The surface wetting condition is commonly measured by the contact angle formed by liquid on a solid surface. The Young's

equation can determine the extent of wetting in terms of the contact angle (θ) and interfacial tension (γ):

$$\cos\theta = \frac{(\gamma_{SV} - \gamma_{SL})}{\gamma_{LV}} \tag{1}$$

where γ_{SV}, γ_{SL} and γ_{LV} are solid–vapor, solid–liquid, and liquid–vapor interfacial tensions, respectively. An important conclusion of this equation is that a liquid with low surface tension is expected to give a small contact angle or completely spread on a solid surface with high energy, such as glasses, metals and oxides. However, some pure organics with low surface tensions form a large contact angle on mica or glass surfaces instead of complete spreading (Fox et al., 1955). Zisman and co-workers noted that some amphiphilic organic compounds with low surface tensions did not completely spread on high-energy solid surfaces (Fox et al., 1955; Hare and Zisman, 1955). An oriented monolayer of amphiphilic molecules forms on the high-energy solid surface because of the sufficiently strong surface interaction between the solid surface and the liquid molecules. This leads to the incomplete spreading of the amphiphilic liquid on its own monolayers, which is called autophobing (Hare and Zisman, 1955; Zisman, 1964). Several studies have been reported in literatures on the autophobing phenomena of amphiphilic organic compounds spreading on a high-energy hydrophilic surface (Afsar-Siddiqui et al., 2003a,b, 2004; Craster and Matar, 2007; Kumar et al., 2003; Sharma et al., 2012). Most of the amphiphilic organics are the key and fundamental components of nonionic surfactants, which are tailed with hydrophobic groups (apolar fatty alkyl chains) but headed with hydrophilic functional groups, such as –OH, –NH$_2$ and –COOH. However, the effects of the functional groups and alkyl groups of these amphiphilic organic compounds on the pore wetting of high-energy hydrophilic surface have not been systematically investigated.

Furthermore, to date, studies of wetting have been limited to observations on flat substrates; few studies were carried in micro-size pores. Pore wetting is a significant factor governing the displacement of two immiscible phases in pores and the transport of multiphase flow in porous materials. Due to lack of a technique for directly measuring the contact angle in a small pore, the pore wetting is often simply estimated by the contact angle measured on a flat substrate (Ameri et al., 2013; Bharatwaj et al., 2007; Broseta et al., 2012; Chiquet et al., 2007; Jung and Wan, 2012; Wang et al., 2012; Yang et al., 2008), which might be relevant in some cases but deserves to be assessed (Gomez et al., 2000; Kim et al., 2012). Thus, we used an experimental apparatus recently used in our laboratory (Li and Fan, 2015; Li et al., 2013, 2014) to directly measure the contact angles of pure organics in a single glass capillary. This paper systematically examines the effects of functional group (–OH, –NH$_2$, –COOH) and the length and structure of alkyl chain of pure amphiphilic organic compounds on their contact angles in a glass pore. The results could significantly advance the understanding of the effects of chemical structure of organic compounds on pore wetting. As well known, the pore wetting is a crucial factor for the estimation of the displacement of oil by water and the oil–water migration in enhanced oil recovery process. The information presented in this paper can give some indications for how chemical structure affects the water-wet pore wetting, further influences the displacement and migration of pore fluids, and the selection of chemicals in surfactant flooding.

2. Experimental methods

2.1. Manufacturing of glass capillary and Cleaning of glass capillary

The glass capillaries with an inner diameter of 250 μm were used in the measurements. They were made from clean glass tubes with O.D. of 6.0 mm and wall thickness of 1.5 mm (Thermo Fisher Scientific UK, TWL-611-010M). The glass tubes were washed by using acetone (Fisher Scientific, A/0600/15), sodium hydroxide solution (Fisher Scientific, 10 M concentrate), concentrated nitric acid solution (Fisher Scientific, 10 M concentrate), and then rinsed thoroughly with deionized water (Fisher and Lark, 1979; Xue et al., 2006). The washed glass tubes were heated up to 550 °C in a flame to remove any residue of organic contamination and were kept in an ash-proof enclosure (Fisher and Lark, 1979). The single capillary was obtained by melting the middle section of dry and clean glass tubes on butane flame (Butane Battery, D2-BS 0167) and drawing the tube to a long distance. The middle section was cut off for the use in this experiment. For each measurement, a new fresh clean capillary was used to avoid prewetting of the capillary interior. In addition, a PMMA (poly(methyl methacrylate)) (Paradigm, CT250-360-5, ID/OD: 250 μm/360 μm) capillary with the same size as the glass capillary was also used. PMMA is hydrophobic and could represent the oil-wet surface.

2.2. X-ray photoelectron spectroscopy (XPS) scanning of glass capillary interiors

To give indicative information on the surface cleanness of the glass capillary interiors used in this study, XPS (X-ray Photoelectron Spectroscopy, Thermofisher, Multilab 2000) was used to check the contamination of the glass capillary inner wall surface by analyzing the chemical composition of the top surface at molecular level and the binding energy. In order to scan the capillary interiors, short sections of glass capillaries were placed between two double-side tapes and crushed (Danisman et al., 2008). The top tape was then removed to ensure the exposed surfaces of the crushed capillaries on the bottom tape facing upwards and representing the inner walls of the capillaries (Li et al., 2013, 2014. The glass capillary interior was scanned and analyzed (Fig. 1). The peaks identified in the spectrum were mainly related to Si(2p), O(1s), Na(1s) and Ca(2p). The surface chemical compositions detected on the glass surfaces were mainly Si, O, Na and Ca (Table 1). The composition of adventitious C was not involved in the XPS surface chemical composition analysis. In addition, our data is similar with the XPS data reported in literature for cleaned soda-lime silicate glass surface (Sharma et al., 2001). Thus, we can conclude that the glass capillary inner surface is no significant measurable chemical contamination.

2.3. Contact angle measurements in a pore

Fig. 2 shows the experimental setup for the contact angle measurement in a single micro-size capillary (Li et al., 2013). The microscopic image of liquid meniscus was obtained by a microscope (Olympus, BHW) equipped with a digital camera (AM7023, Dino-Eye). Since the quality of meniscus image of the small volume of liquid in a capillary highly depends on the light source and measurement method, a LED light source located under the glass capillary was used for the microscopic imaging to improve the quality of image. The LED light travels from the liquid end up to the meniscus in a dark background to overcome the degree of image distortion problem when a cylindrical capillary is used and therefore facilitate the measurements (Cheong et al., 2011). The outermost boundary of liquid–gas interface was well lit and focused to produce the clear two-phase interface. This is similar to the principle used in measuring micron air-bubble size (Fan et al., 2004), micron ice crystal size in aqueous solution (Fan et al., 2003), and the size of a plant cell or a microcapsule in water under a microscope (Rosiñski et al., 2002).

The experiments were started by placing a single capillary onto a cleaned glass slide. A small amount of liquid of 0.5–1 μL was dropped onto one end of the capillary by a microfluidics syringe
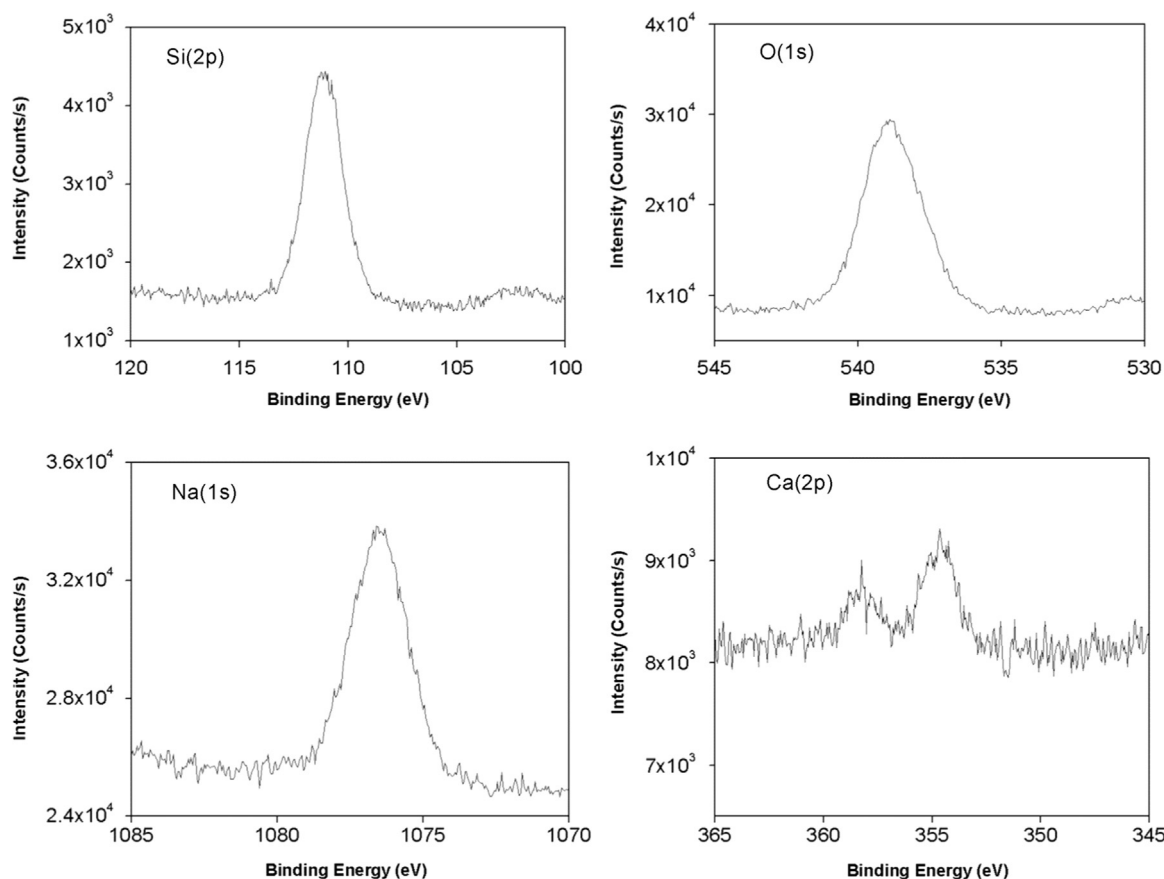
Fig. 1. XPS spectra of glass capillary interior (Li et al., 2014).

Table 1
Surface chemical composition of glass capillary interior (Li et al., 2014).

Element	Atomic percentage (%)	
	Glass capillary interior	Sharma et al. (2001)
Si	25.9	26.0
O	61.2	61.0
Ca	2.8	3.6
Na	10.0	9.5

Fig. 2. Experimental setup for the study of the contact angle in a capillary. (the vector $\overline{\mathbf{g}}$ shows the direction of gravity) (Li et al., 2013).

(Hamilton, 701ASN 10 μL). The liquid was then imbibed into the capillary by its own capillary pressure at ambient conditions. When the imbibition and any dynamic movement of liquid

completely stopped and the equilibrium status of liquid in a capillary was reached, the image of the meniscus was taken and analyzed. Each measurement was repeated up to five times to confirm the reliability of experimental data.

In order to obtain the contact angle of liquid in a capillary, we analyzed the microscopic images by using the method recently proposed by Cheong et al. (2011). The contact angle of liquid in a capillary was calculated by only using the capillary radius (r) and meniscus height (h) (Fig. 2) of the capillary meniscus as shown in (Eq. (2)). This equation is valid based on the assumptions of small liquid volume applied and neglected gravity effect (Cheong et al., 2011; Zheng et al., 2005). Since the effect of image distortion on meniscus height (h) is not significant, the effect of image distortion on contact angle estimation of liquid in a small pore can be minimized (Cheong et al., 2011).

$$\theta = \tan^{-1}\left(\frac{r^2 - h^2}{2rh}\right) \qquad (2)$$

In order to investigate the effect of chemical structure of organic compounds on pore contact angle, a variety of organics were used to examine the effects of functional group and alkyl chain on pore wetting, such as the non-polar saturated alkanes (Pentane, Hexane, Octane and Decane), and amphiphilic organic compounds, tailed with straight-chain hydrophobic alkyl groups of different chain length ($(CH_3)_n-$), $n=1,2,3,4,6,8,10$) and headed with hydrophilic functional groups ($-OH$, $-NH_2$ and $-COOH$). The structural isomers of 1-propanol and 1-butanol, namely, 2-propanol, *tert*-butanol, 2-butanol and 2-methyl-1-propanol, were used to investigate the effect of alkyl chain structure on the pore wetting. In addition to the alkanols with only one hydroxyl group, ethylene glycol and glycerol with two and three hydroxyl groups
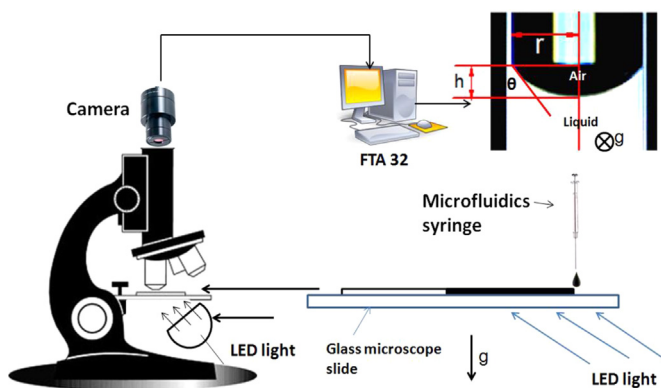
were also used to explore the effect of the multiple hydroxyls on the alkyl backbone chain on pore wetting.

The physical properties and structural features of all the organic compounds used in this study are shown in Table 2. The surface tensions of liquids were determined by pendant drop experiments (First Ten Angstroms).

3. Results and discussion

Fig. 3 shows the contact angles in a glass pore for the organics used in this study as well as their surface tensions. The results indicate that contact angle varies with the chemical molecular structures of organics. The organic liquids in this study have similar surface tensions ($\sim$20 mN/m), but their contact angles do vary significantly with the functional groups and the arrangement of carbons in the alkyl chain. The change in contact angle is not always proportional to the change in liquid surface tension. Alkanols, alkylamines and alkyl carboxyl acids have similar surface tensions, but some of them give very different contact angles. The alkanols, alkyl amines and alkyl carboxyl acids with an alkyl chain over 4 carbon atoms give contact angles over 40°. While the contact angles of short-chain amphiphilic organic compounds stay around 30°.

The large contact angles of long-chain amphiphilic organic compounds in a glass pore might be caused by the adsorbed oriented amphiphile layers on the high-energy surface, which is
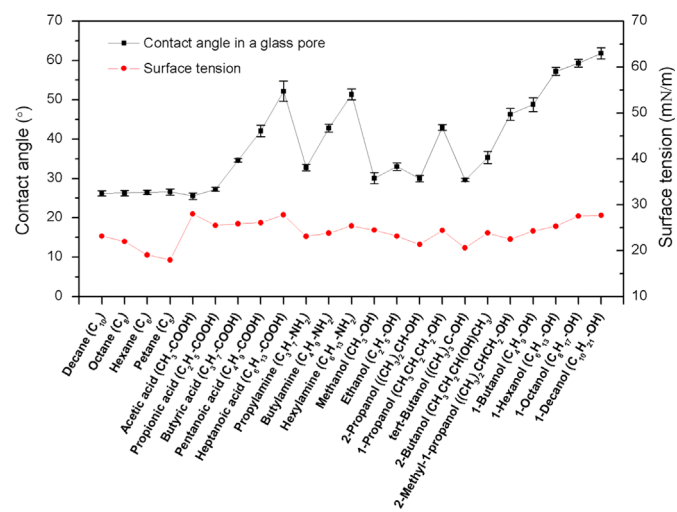

Fig. 3. Contact angles in a glass pore and the surface tensions for the organics used in this study.

Table 2
The physical and structural properties of liquids investigated.

Liquids	Density (kg/m³)	Surface tension (mN/m)	Vapor[a] pressure (kPa)	Molecular weight (g/mol)	Chemical formula	Molecular structure
Pentane	626.0	18.0	56.5	72.2	C_5H_{12}	
Hexane	654.8	19.0	16.2	86.2	C_6H_{14}	
Octane	703.0	22.0	1.3	114.2	C_8H_{18}	
Decane	730.0	23.2	9.5×10^{-2}	142.3	$C_{10}H_{22}$	
Propionic acid	990.0	25.5	0.4	74.1	$C_3H_6O_2$	
Butyric acid	959.5	25.9	0.1	88.1	$C_4H_8O_2$	
Pentanoic acid	930.0	26.1	8.5×10^{-3}	102.1	$C_5H_{10}O_2$	
Heptanoic acid	918.1	27.8	2.8×10^{-4}	130.2	$C_7H_{14}O_2$	
Propylamine	719.0	23.1	33.8	59.1	C_3H_9N	
Butylamine	740.0	23.8	9.1	73.1	$C_4H_{11}N$	
Hexylamine	766.0	25.4	0.9	101.2	$C_6H_{15}N$	
Methanol	791.8	24.5	13.0	32.0	CH_4O	
Ethanol	789.0	23.1	5.9	46.1	C_2H_6O	
1-Propanol	803.4	24.4	2.0	60.1	C_3H_8O	
2-Propanol	786.0	21.3	4.2	60.1	C_3H_8O	
1-Butanol	810.0	24.3	0.6	74.1	$C_4H_{10}O$	
2-Methyl-1-propanol	802.0	22.5	0.9	74.1	$C_4H_{10}O$	
2-Butanol	806.3	23.9	1.5	74.1	$C_4H_{10}O$	
tert-Butanol	780.9	20.6	4.0	74.1	$C_4H_{10}O$	
1-Hexanol	814.0	25.3	5.6×10^{-2}	102.2	$C_6H_{14}O$	
1-Octanol	827.0	27.5	6.6×10^{-3}	130.2	$C_8H_{18}O$	
1-Decanol	829.0	27.7	5.5×10^{-4}	158.3	$C_{10}H_{22}O$	
Ethylene glycol	1110.0	47.9	1.1×10^{-2}	62.1	$C_2H_6O_2$	
Glycerol	1260.0	63.1	1.3×10^{-4}	92.1	$C_3H_8O_3$	

[a] The vapor pressures were calculated by Antoine equation ($\log_{10}(P) = A - (B/(T+C))$) at 20 °C. The A, B and C are Antoine equation parameters taken from NIST Chemistry WebBook (NIST, 2005).

called autophobing (Afsar-Siddiqui et al., 2003a,b, 2004; Atkin and Warr, 2007; Craster and Matar, 2007; Frank and Garoff, 1995, 1996; Kumar et al., 2003; Novotny and Marmur, 1991; Qu et al., 2002; Sharma et al., 2012; Souda, 2012). Several organics with low surface tensions have been reported that they cannot spread completely on high energy solid surfaces under their own saturated vapor (Fox et al., 1955; Hare and Zisman, 1955; Zisman, 1964). The adsorbed amphiphile molecules make the solid–vapor interfacial tension (γ_{SV}) to be lower than the solid–vacuum interfacial tension (γ_S), and thus render in incomplete spreading and raising the contact angle of the drop (Frank and Garoff, 1995; Kwok and Neumann, 2000; Novotny and Marmur, 1991).

In addition, the pore contact angles of all the amphiphiles used in this study were also measured in a PMMA (polymethyl methacrylate) capillary, and compared with those in a glass capillary in Fig. 4. PMMA is hydrophobic, oil-wet and has a low surface energy ($\gamma_S \approx 38$ mN/m) (Kwok and Neumann, 2000). The results indicate that all the liquids give a similar and small contact angle of 20°. The wetting behaviour of amphiphilic organic compounds in an oil-wet pore is not significantly related to the molecular structure and functional group of amphiphile.

Novotny and Marmur (1991) demonstrated that the amphiphile vapor film formation mechanism was the evaporation followed by adsorption rather than surface diffusion. As the amphiphile layer is formed by evaporation, the vapor pressure of amphiphile must be considered as one of the important factors in this study. However, our results in Fig. 5 show that the contact angles of alkanols, alkylamines and alkyl carboxyl acids do not clearly relate to their vapor pressures. Novotny and Marmur (1991) suggested that the adsorbed vapor film could be mainly controlled by the adsorption characteristics of the amphiphile molecules rather than vapor pressure. In Fig. 5, we also noticed that the pore contact angles given by the amphiphiles vary greatly with molecular structure and molecular weight. The effect of molecular structure on contact angle would be complex. In the following sections, the effects of functional group and alkyl chain of amphiphiles on the glass pore wetting will be discussed separately.

Fig. 6 presents the pore contact angles of three amphiphilic organics with the same alkyl chain length (number of carbon atoms is 3) but with different hydrophilic functional groups, namely, carboxyl (–COOH), amino (–NH₂), and hydroxyl (–OH) groups. They are used to investigate the effect of functional group
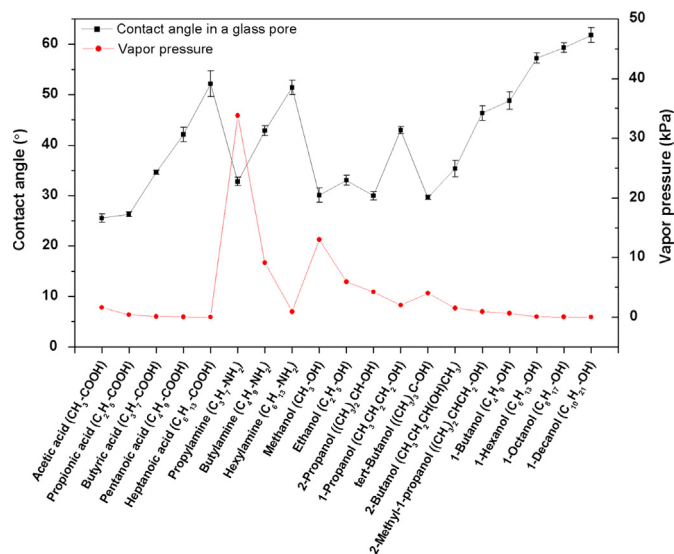

Fig. 5. Contact angles in a pore and vapor pressures at 20 °C for all amphiphiles used in this study.
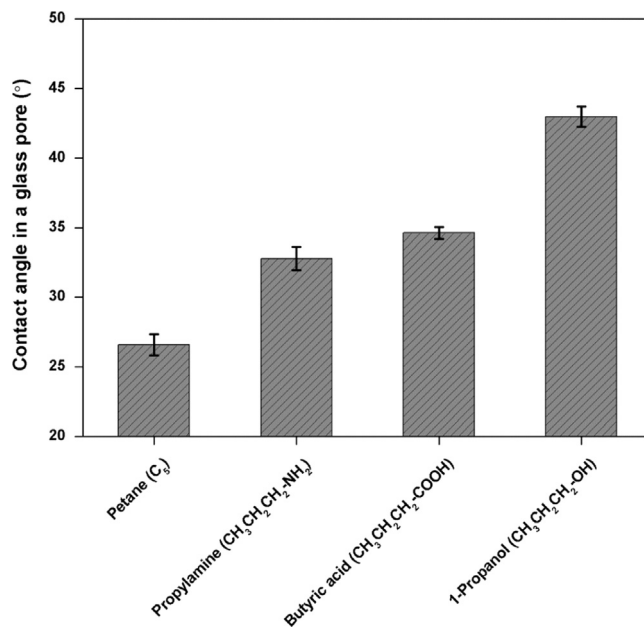

Fig. 6. Pore contact angles of pentane, propionic acid, propylamine and 1-propanol.

on glass pore wetting. The results indicate that the effect of function group on contact angle in a glass pore is in the order of $\theta_{-OH} > \theta_{-COOH} \approx \theta_{-NH_2}$, but their surface tensions are similar around 20 mN/m. Pentane and 1-propanol have the lowest and largest pore contact angles, which are 26.6° and 43.0°, respectively. Similar pore contact angles given by propylamine and butyric acid are around 34°. The amphiphilic organics with functional groups have larger pore contact angles than that of nonpolar alkane.

The results in Fig. 7 further demonstrate the effect of functional group and also indicate the effect of straight alkyl chain length on glass pore wetting. It clearly shows that the contribution of the studied functional groups to the glass pore wetting is in the order: alkanol > alkyl amines ≈ alkyl carboxyl acid. For the saturated alkanes, the pore contact angle does not vary with the length of alkyl chain. The pore contact angles of pentane, hexane, octane and decane remains at around 26°. However, once a polar functional group is introduced to the molecules, the pore contact angle increased significantly with the alkyl chain length. For instance,
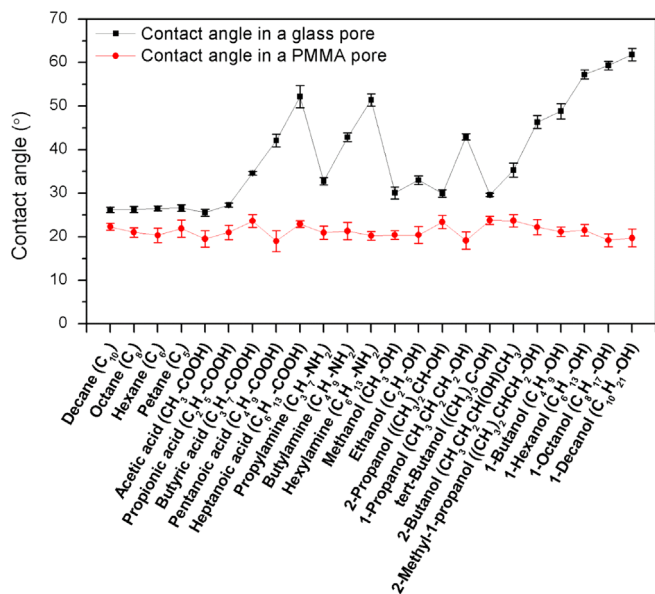

Fig. 4. Comparison of contact angles measured in a glass pore and a PMMA pore.
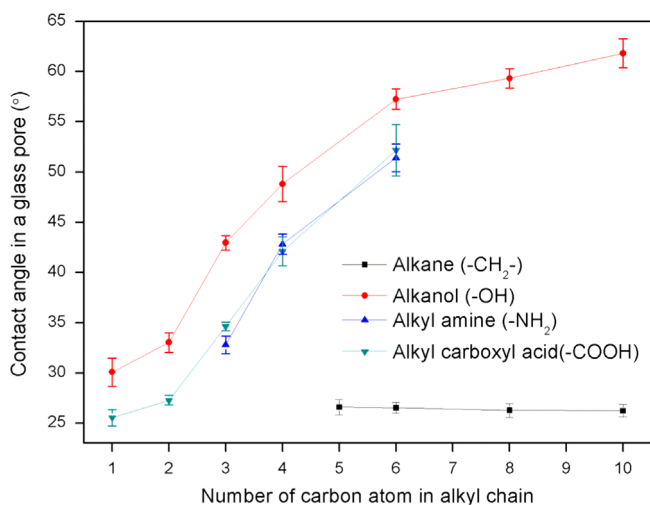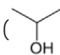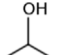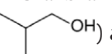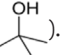
Fig. 7. Pore contact angles of alkanes, alkanols, alkylamines and alkyl carboxyl acid with different straight alkyl chain lengths.

Fig. 8. Pore contact angles of structural isomers of 1-propanol and 1-butanol.

the pore contact angle of ethanol is larger than that from methanol by 3°. The effect of the alkyl chain length becomes more significant when the number of carbon atoms in straight alkyl chain increases from 3 to 6. The pore contact angle of 1-hexanol ($C_6H_{13}OH$) is larger than that from 1-propanol (C_3H_7OH) by 14°. The contact angles of alkylamines and alkyl carboxyl acids are similar at the same alkyl chain length. They are smaller than the contact angles from alkanol, by around 6–10°. However, the dependence of glass pore contact angle on the alkyl chain length for alkylamines and alkyl carboxyl acids is consistent with that for alkanols in the alkyl chain length range from 1 to 6. When the number of carbon atoms in the alkyl chain is more than 6, the pore contact angle of alkanols increases with the alkyl chain length less significantly. The difference between the pore contact angles of 1-decanol ($C_{10}H_{21}OH$) and 1-hexanol ($C_6H_{13}OH$) is only 5°. Alkyl amines and alkyl carboxyl acid with carbons over 6 are solids. Methylamine and ethylamine are gas at ambient conditions. Thus, they were not involved in this study.

To investigate the effect of the alkyl chain structure of the amphiphilic organic compounds on pore contact angle, the structural isomers of 1-propanol and 1-butanol were used in this study. 2-propanol is the only structural isomer of 1-propanol. Its alcohol carbon is attached to two other carbons ( ). 1-Butanol has three structural isomers, which are 2-butanol, 2-methyl-1-propanol and *tert*-butanol. 2-Butanol is a straight chain isomer with the hydroxyl at an internal carbon ( ), 2-methyl-1-propanol is a branched isomer with the hydroxyl at a terminal carbon ( ) and *tert*-butanol is a branched isomer with the hydroxyl at the internal carbon ( ). From Fig. 8, the difference in pore contact angle between 1-propanol and 2-propanol is 12°. This is caused by the different propyl chains of 1-propanol and 2-propanol. The straight *n*-propyl chain of 1-propanol gives larger pore contact angle than that given by the isopropyl of 2-propanol, by 13°. Similarly, the structural isomers of 1-butanol also give various pore contact angles. The straight *n*-butyl chain of 1-butanol gives the largest pore contact angle of 49°. The pore contact angles of 2-methyl-1-propanol and 2-butanol are smaller, which are 46° and 35°, respectively. This is caused by the effects of the isobutyl group of 2-methyl-1-propanol and the *sec*-butyl group of 2-butanol. The difference between isobutyl and *sec*-butyl group
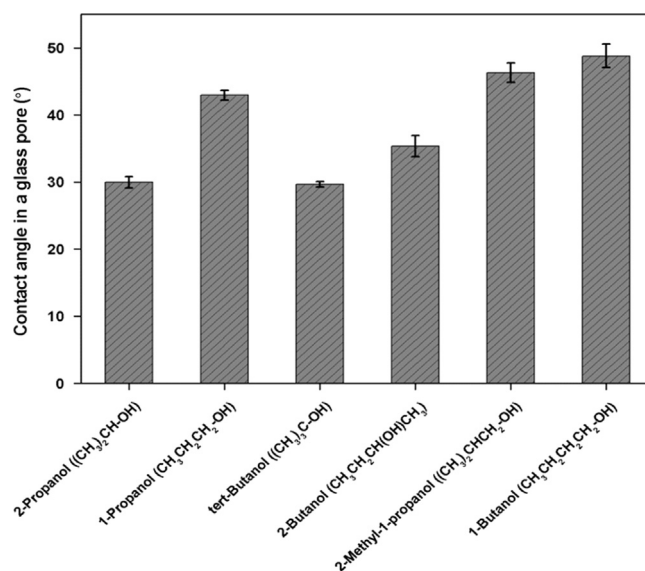
is the location of methyl side chain. The methyl side chain on the alcohol carbon tends to reduce the pore contact angle more significantly than the methyl side chain on internal carbon. The pore contact angle of *tert*-butanol is the smallest, which is only around 29°. This is due to the two methyl side chains on the alcohol carbon and the shortest backbone chain. Overall, it can be concluded that the structure of alkyl chain of amphiphilic organic compounds has a significant effect on the glass pore wetting. The straight alkyl chain favors the pore contact angle most and the side chain on carbon of backbone tends to reduce the pore contact angle, and the side chain on the alcohol carbon decreases the pore contact angle most significantly.

The effect of hydroxyl on the pore contact angle discussed in Figs. 7 and 8 was investigated by using the alkanols with only one hydroxyl located on the terminal carbon, such as ethanol and 1-propanol. The alkanol with a single hydroxyl has a larger pore contact angle than the alkane with the same chain length. To investigate the effect of multiple hydroxyls on pore wetting of alkanols, ethylene glycol and glycerol were used. They have the same number of carbons as the ethanol and 1-propanol but have two and three hydroxyls on all carbons of their backbone chains, respectively. In Fig. 9, the pore contact angles of ethylene glycol and glycerol are smaller than those from ethanol and 1-propanol by 4.5° and 17°, respectively. The pore contact angle is not increased by increasing the number of hydroxyls in the alkanols. Instead, the pore contact angle is significantly reduced due to the symmetrical molecular structure formed by introducing more hydroxyl functional groups on the backbone chain carbons.

4. Conclusions

Pore contact angle is an important factor for the multiphase flow transport in porous media. In this study, the contact angles of a range of organic compounds were directly measured in a glass micron-sized pore by the pore contact angle measurement technique we recently used (Li and Fan, 2015; Li et al., 2013, 2014). We investigated the effect of chemical structure of organics on glass pore wetting in terms of functional group, alkyl chain length and chain structural isomer. The main results indicate the following.

Contact angle of organics in a glass pore not only depends on their surface tension but also on their chemical structure. Some organics have very small and similar surface tensions, but their
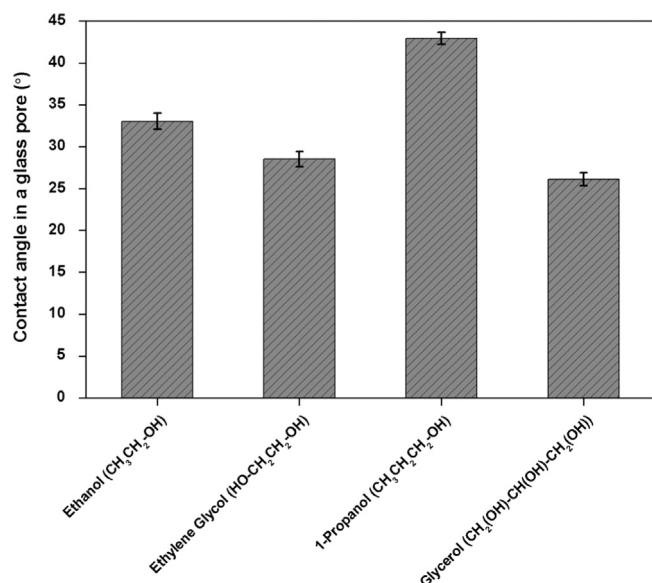
Fig. 9. The pore contact angles of ethanol, ethylene glycol, 1-propanol and glycerol.

contact angles are large and very different in a glass pore due to the contributions from the effects of functional groups, alkyl chain length and alkyl chain structure. However, the chemical structure of amphiphile only affects the contact angle in a hydrophilic glass pore. The findings cannot be applied to the hydrophobic oil-wet surface.

The amphiphilic organics with functional groups of hydroxyl, amino and carboxyl have larger pore contact angles than the non-polar organics, and in the order of $\theta_{-OH} > \theta_{-NH_2} \approx \theta_{-COOH}$. The pore contact angle of amphiphiles increases with the straight alkyl chain length. However, the pore contact angle of non-polar organics does not depend on the alkyl chain length. The structure of alkyl chain of amphiphilic compounds also has an effect on the glass pore wetting. The straight alkyl chain contributes to the pore contact angle most and the side chain on the carbon of backbone tends to reduce the pore contact angle. The symmetrical molecular structure of organic gives the smallest contribution on the pore wetting. In the future, we will also investigate the contact angle from the imbibition height of the liquid in a capillary.

Acknowledgements

References

Afsar-Siddiqui, A.B., Luckham, P.F., Matar, O.K., 2003a. Unstable spreading of aqueous anionic surfactant solutions on liquid films. 2. Highly soluble surfactant. Langmuir 19, 703–708.

Afsar-Siddiqui, A.B., Luckham, P.F., Matar, O.K., 2003b. Unstable spreading of aqueous anionic surfactant solutions on liquid films. Part 1. Sparingly soluble surfactant. Langmuir 19, 696–702.

Afsar-Siddiqui, A.B., Luckham, P.F., Matar, O.K., 2004. Dewetting behavior of aqueous cationic surfactant solutions on liquid films. Langmuir 20, 7575–7582.

Altman, S.J., Aminzadeh, B., Balhoff, M.T., Bennett, P.C., Bryant, S.L., Cardenas, M.B., Chaudhary, K., Cygan, R.T., Deng, W., Dewers, T., DiCarlo, D.A., Eichhubl, P.,

Hesse, H., Huh, C., Matteo, E.N., Mehmani, Y., Tenney, C.M., Yoon, H., 2014. Chemical and hydrodynamic mechanisms for long-term geological carbon storage. J. Phys. Chem. C 118, 15103–15113.

Ameri, A., Kaveh, N.S., Rudolph, E.S.J., Wolf, K.H., Farajzadeh, R., Bruining, J., 2013. Investigation on interfacial interactions among crude oil–brine–sandstone rock–CO_2 by contact angle measurements. Energy Fuels 27, 1015–1025.

Atkin, R., Warr, G.G., 2007. Structure in confined room-temperature ionic liquids. J. Phys. Chem. C 111, 5162–5168.

Bharatwaj, B., Wu, L., da Rocha, S.R.P., 2007. Biocompatible, lactide-based surfactants for the CO_2 – iocompatible, la high-pressure contact angle goniometry, tensiometry, and emulsion formation. Langmuir 23, 12071–12078.

Bikkina, P.K., 2011. Contact angle measurements of CO_2–water–quartz/calcite systems in the perspective of carbon sequestration. Int. J. Greenhouse Gas Control 5, 1259–1271.

Broseta, D., Tonnet, N., Shah, V., 2012. Are rocks still water-wet in the presence of dense CO_2 or H_2S? Geofluids 12, 280–294.

Brovchenko, I., Oleinikova, A., 2011. Effect of pore size on the condensation/ evaporation transition of confined water in equilibrium with saturated bulk water. J. Phys. Chem. B 115, 9990–10000.

Chalbaud, C., Robin, M., Lombard, J.M., Martin, F., Egermann, P., Bertin, H., 2009. Interfacial tension measurements and wettability evaluation for geological CO_2 storage. Adv. Water Resour. 32, 98–109.

Cheong, B.H.-P., Ng, T.W., Yu, Y., Liew, O.W., 2011. Using the meniscus in a capillary for small volume contact angle measurement in biochemical applications. Langmuir 27, 11925–11929.

Chiquet, P., Broseta, D., Thibeau, S., 2007. Wettability alteration of caprock minerals by carbon dioxide. Geofluids 7, 112–122.

Craster, R.V., Matar, O.K., 2007. On autophobing in surfactant-driven thin films. Langmuir 23, 2588–2601.

Danisman, M.F., Calkins, J.A., Sazio, P.J.A., Allara, D.L., Badding, J.V., 2008. Organosilane self-assembled monolayer growth from supercritical carbon dioxide in microstructured optical fiber capillary arrays. Langmuir 24, 3636–3644.

Ersland, G., Fernø, M.A., Graue, A., Baldwin, B.A., Stevens, J., 2010. Complementary imaging of oil recovery mechanisms in fractured reservoirs. Chem. Eng. J. 158, 32–38.

Espinoza, D.N., Santamarina, J.C., 2010. Water–CO_2–mineral systems: interfacial tension, contact angle, and diffusion—implications to CO_2 geological storage. Water Resour. Res. 46, W07537.

Fan, X., Ten, P., Clarke, C., Bramley, A., Zhang, Z., 2003. Direct measurement of the adhesive force between ice particles by micromanipulation. Powder Technol. 131, 105–110.

Fan, X., Zhang, Z., Li, G., Rowson, N.A., 2004. Attachment of solid particles to air bubbles in surfactant-free aqueous solutions. Chem. Eng. Sci. 59, 2639–2645.

Fisher, L.R., Lark, P.D., 1979. An experimental study of the washburn equation for liquid flow in very fine capillaries. J. Colloid Interface Sci. 69, 486–492.

Fox, H.W., Hare, E.F., Zisman, W.A., 1955. Wetting properties of organic liquids on high energy surfaces. J. Phys. Chem. 59, 1097–1106.

Frank, B., Garoff, S., 1995. Temporal and spatial development of surfactant self-assemblies controlling spreading of surfactant solutions. Langmuir 11, 4333–4340.

Frank, B., Garoff, S., 1996. Surfactant self-assembly near contact lines: control of advancing surfactant solutions. Colloids Surf., A: Physicochem. Eng. Aspects 116, 31–42.

Gomez, F., Denoyel, R., Rouquerol, J., 2000. Determining the contact angle of a nonwetting liquid in pores by liquid intrusion calorimetry. Langmuir 16, 4374–4379.

Hare, E.F., Zisman, W.A., 1955. Autophobic liquids and the properties of their adsorbed films. J. Phys. Chem. 59, 335–340.

Hui, M.-H., Blunt, M.J., 2000. Effects of wettability on three-phase flow in porous media. J. Phys. Chem. B 104, 3833–3845.

Jung, J.-W., Wan, J., 2012. Supercritical CO_2 and ionic strength effects on wettability of silica surfaces: equilibrium contact angle measurements. Energy Fuels 26, 6053–6059.

Kim, Y., Wan, J., Kneafsey, T.J., Tokunaga, T.K., 2012. Dewetting of silica surfaces upon reactions with supercritical CO_2 and brine: pore-scale studies in micromodels. Environ. Sci. Technol. 46, 4228–4235.

Kumar, N., Varanasi, K., Tilton, R.D., Garoff, S., 2003. Surfactant self-assembly ahead of the contact line on a hydrophobic surface and its implications for wetting. Langmuir 19, 5366–5373.

Kwok, D.Y., Neumann, A.W., 2000. Contact angle interpretation in terms of solid surface tension. Colloids Surf., A: Physicochem. Eng. Aspects 161, 31–48.

Li, X., Fan, X., 2015. Effect of CO_2 phase on contact angle in oil-wet and water-wet pores. Int. J. Greenhouse Gas Control 36, 106–113.

Li, X., Fan, X., Askounis, A., Wu, K., Sefiane, K., Koutsos, V., 2013. An experimental study on dynamic pore wettability. Chem. Eng. Sci. 104, 988–997.

Li, X., Fan, X., Brandani, S., 2014. Difference in pore contact angle and the contact angle measured on a flat surface and in an open space. Chem. Eng. Sci. 117, 137–145.

Martic, G., Blake, T.D., De Coninck, J., 2005. Dynamics of imbibition into a pore with a heterogeneous surface. Langmuir 21, 11201–11207.

NIST, 2005. NIST Chemistry WebBook, NIST Standard Reference Database Number 69. National Institute of Standards and Technology.

Novotny, V.J., Marmur, A., 1991. Wetting autophobicity. J. Colloid Interface Sci. 145, 355–361.

Qu, D., Suter, R., Garoff, S., 2002. Surfactant self-assemblies controlling spontaneous dewetting. Langmuir 18, 1649–1654.

Raimondo, M., Blosi, M., Caldarelli, A., Guarini, G., Veronesi, F., 2014. Wetting behavior and remarkable durability of amphiphobic aluminum alloys surfaces in a wide range of environmental conditions. Chem. Eng. J. 258, 101–109.

Rosiński, S., Grigorescu, G., Lewińska, D., Ritzén, L.G., Viernstein, H., Teunou, E., Poncelet, D., Zhang, Z., Fan, X., Serp, D., Marison, I., Hunkeler, D., 2002. Characterization of microcapsules: recommended methods based on round-robin testing. J. Microencapsul. 19, 641–659.

Saraji, S., Goual, L., Piri, M., Plancher, H., 2013. Wettability of supercritical carbon dioxide/water/quartz systems: simultaneous measurement of contact angle and interfacial tension at reservoir conditions. Langmuir 29, 6856–6866.

Sghaier, N., Prat, M., Ben Nasrallah, S., 2006. On the influence of sodium chloride concentration on equilibrium contact angle. Chem. Eng. J. 122, 47–53.

Sharma, A., Jain, H., Miller, A.C., 2001. Surface modification of a silicate glass during XPS experiments. Surf. Interface Anal. 31, 369–374.

Sharma, R., Kalita, R., Swanson, E.R., Corcoran, T.E., Garoff, S., Przybycien, T.M., Tilton, R.D., 2012. Autophobing on liquid subphases driven by the interfacial transport of amphiphilic molecules. Langmuir 28, 15212–15221.

Souda, R., 2012. Nanoconfinement effects on the glass–liquid transition of vapor-deposited 1-pentene. J. Phys. Chem. C 116, 7735–7740.

Stukan, M.R., Ligneul, P., Crawshaw, J.P., Boek, E.S., 2010. Spontaneous imbibition in nanopores of different roughness and wettability. Langmuir 26, 13342–13352.

Vanzo, D., Bratko, D., Luzar, A., 2014. Dynamic control of nanopore wetting in water and saline solutions under electric field. J. Phys. Chem. B.

Wang, S., Edwards, I.M., Clarens, A.F., 2012. Wettability phenomena at the CO_2–brine–mineral interface: implications for geologic carbon sequestration. Environ. Sci. Technol. 47, 234–241.

Xue, H.T., Fang, Z.N., Yang, Y., Huang, J.P., Zhou, L.W., 2006. Contact angle determined by spontaneous dynamic capillary rises with hydrostatic effects: experiment and theory. Chem. Phys. Lett. 432, 326–330.

Yang, D., Gu, Y., Tontiwachwuthikul, P., 2008. Wettability determination of the crude oil-reservoir brine-reservoir rock system with dissolution of CO_2 at high pressures and elevated temperatures. Energy Fuels 22, 2362–2371.

Zheng, Q.S., Yu, Y., Zhao, Z.H., 2005. Effects of hydraulic pressure on the stability and transition of wetting modes of superhydrophobic surfaces. Langmuir 21, 12207–12212.

Zisman, W.A., 1964. Relation of the Equilibrium Contact Angle to Liquid and Solid Constitution, Contact Angle, Wettability, and Adhesion. American Chemical Society, pp. 1–51.